

## FLOW CHARACTERISTICS OF PARTIALLY VEGETATED TRAPEZOIDAL CHANNEL CROSS-SECTION WITH FLEXIBLE VEGETATION

Hassan I. Mohamed

Associate Prof., Civil Eng. Department, Assiut University, Assiut, Egypt

E-mail: [hassanmohamed\\_2000@yahoo.com](mailto:hassanmohamed_2000@yahoo.com)

### ABSTRACT

An important feature of most rivers and canals is their habitats for a rich of aquatic vegetation which is extremely important from an environmental and ecological point of view. These variations in habitat mean that it is rare to find a cross-section of a natural channel which has the same roughness along its perimeter. In these channels, flow conditions lead to a complex flow situation with intensive mass and momentum exchange between main channel and banks, and secondary currents. Therefore the flow structures that occur in these channels are extremely complex. In this research, a method for predicting the total conveyance of trapezoidal channel cross-section with varying roughness in perimeter due to growth of flexible vegetation is developed based on the 2D velocity distribution in open channel. Where, numerical hydraulic model is coupled with physically based flexible vegetation flow-resistance equation. The study covers three patterns of flexible vegetation growth, the first is vegetation growth on bed and side banks with equal height on both, the second is vegetation growth on bed only and sediment roughness on side banks and the third is vegetation growth on side banks and alluvial on the bed. The resulting model is capable of simulating the total conveyance of trapezoidal channels with growth of vegetation on bed and/or side banks, depth average velocity distribution and bed shear stress distribution along the channel cross-section. From the numerical results, series of regression relationships were developed for computing the equivalent Manning coefficient for vegetated channels and another series were developed for computing the vegetated channel flow rate. These can be used as an alternative solution for channel designs; relieving the practitioner of the need to run the numerical program. A comparison between the present method and traditional empirical approaches proved that the model is superior on the other methods. The flow capacity results obtained are shown to be in good agreement with actual field data, as are the equivalent Manning's roughness coefficient.

**Keywords:** Flexible vegetation, Momentum transfer, Flow conveyance

### NOMENCLATURE

The following symbols are used in this paper:

$B$  = top width of the channel;

- $b$  = bottom width of the channel;  
 $f$  = Darcy-Weisbach friction factor;  
 $g$  = gravity of acceleration;  
 $h_b$  = bed vegetation height;  
 $h_s$  = side banks vegetation height;  
 $k$  = local roughness height;  
 $M$  = stem density;  
 $MEI$  = vegetation stiffness parameter (flexible vegetation);  
 $NEV$  = non-dimensional eddy viscosity coefficient;  
 $q$  = discharge per unit width;  
 $S$  = longitudinal channel bed slope;  
 $S_y$  = side slope of the channel;  
 $S_0$  = longitudinal channel slope at no vegetation;  
 $u$  = mean stream wise velocity through the element;  
 $y$  = co-ordinate in the transverse direction;  
 $z$  = local water depth through the element;  
 $\varepsilon$  = eddy viscosity;  
 $\mu$  = absolute viscosity;  
 $\rho$  = water density; and  
 $\tau_{xy}$  = lateral shear stress.

## 1. INTRODUCTION

Situations where channels sections have roughness varying laterally along the wetted perimeter are often encountered in design problems and laboratory experiments. Canals and tunnels partly lined with different construction materials in bottom and sides, highly vegetated sides with smooth channel bed, and over-banks with varying land use and treatment under high stages are the typical instances, Mohamed [1], Bakry [2]. If such types of channels are designed by the traditional methods (averaged cross sectional parameters), this will expose these channels to expensive and environmentally damaging. In all such problems, computations of equivalent roughness for the whole section are sometimes necessary. Various formulas to compute this equivalent or composite roughness can be found in the literature, Bakry [3], Salama and Bakry [4], U.S. Army Corps of Engineers [5], Armanini and Righetti [6] and Garbrecht and Brown [7].

Recent researches have shown that the use of channel with varying roughness as a single unit will underestimate the values of discharge which obtained, Myers et al. [8]. This because the method used ignores the turbulent shear interaction and momentum transfer between the bed and side banks. The turbulent shear (forming vortices) that transfer momentum away from the bed to the banks has been thoroughly investigated by Rabkova and Garanina [9], where they measured the three-dimensional components of velocity in trapezoidal cross section and confirmed kinetic energy exchange

between adjacent layers. They concluded that this process controls the formation of longitudinal velocities in the water column. It is common knowledge that characteristic features of the turbulent flow are velocity fluctuations and the vortex motion, which results in the formation of three-dimensional vortices. The displacement of these vortices brings about redistribution of kinetic energy between elements of the liquid. This process is especially active in the zones, where local velocities vary because of variations in the depth or bed roughness. Under the effect of transverse circulation, the accelerated liquid intrudes into the near bottom layers and vice versa. The result is the general levelling of three-dimensional flow velocity both in the vertical and transverse direction. Liao and Knight [10, 11] developed analytic stage discharge formulas for rectangular and trapezoidal open channel based on the 2D analytic velocity distribution in open channels. However, the main limitation of their approach is the complexity of the algebra when the cross-section is divided into multiple panels or there is a variation in roughness along the channel cross-section. Zarrati et al. [12] derived semi analytical equation for distribution of shear stress in straight open channel with rectangular, trapezoidal, and compound cross sections. However, these equations are limited to homogenous roughness distribution on the wetted periphery. Moreover, Lim and Yang [13] developed an analytical method for the computation of boundary shear stress distribution acting on the flow perimeter of closed ducts. The approach assumes that the surplus energy for any unit volume of fluid in 3D flow will be transferred to the nearest boundary to be dissipated.

To this date, however, very little has been done to evaluate unique model using numerical and mathematical base. As shown from the mentioned above, there are clear needs for physically based methods of predicting the impacts of partially growth of vegetation on flow resistance and flow capacity. In the following, a numerical hydraulic model will be coupled with flow resistance equations for computing flow in channels with varying vegetation growth along the channel cross-section.

## 2. THEORETICAL CONSIDERATION

As, it is shown above, the flow in open channels is accompanied by momentum transfer perpendicular to the main flow direction and this will be more effective in the case of variation in the roughness through the wetted perimeter due to the turbulent interaction between the fluid streams. Observation of depth average velocity distributions, such as those shown in Rabkova and Garanina [9] illustrates that there is a transition between the main channel and banks velocities that can not be dealt with by applying an apparent shear stress at a single interface. Rather, there is a variation of the apparent lateral shear stress ( $\tau_{xy}$ ) across the channel. To better model this variation of the apparent shear stress, Lambert and Sellin [14]; Darby and Thorne [15]; Darby [16], (which is a representation of the turbulent momentum exchange  $\rho \cdot u' \cdot v'$ , where  $u'$  is the fluctuating downstream velocity and  $v'$  is the fluctuating cross-stream velocity) the channel can be subdivided into a finite number of vertical elements as shown in Fig. (1). The vertical element is examined in more detail, using the control volume as in Fig. (1-b) for uniform flow, it can be shown that;

$$gSz - B_* \frac{\tau_b}{\rho} + \frac{1}{\rho} \frac{\partial(z\tau_{xy})}{\partial y} = 0 \quad (1)$$

where  $S$  is the longitudinal channel slope,  $z$  is the local depth measured normal to the channel bed,  $\tau_{xy}$  is the lateral shear stress and  $\tau_b$  is the bed shear stress. The coefficient ( $B_*$ ) associated with the bed shear stress is used to account for the increased area of contact with the channel bed due to the lateral inclination of the channel bed at a cross-section ( $S_y$ ) and is equal to  $\sqrt{1+S_y^2}$ . A factor similar to ( $B_*$ ) was first introduced by both Lambert and Sellin [14]; Darby and Thorne [15]; Darby [16]. This approach to the derivation of Eqn. (1) was chosen because of its ease and accessibility. The solution of Eqn. (1) and in particular the evaluation of the apparent lateral shear stress ( $\tau_{xy}$ ) and the bed shear stress ( $\tau_b$ ) are detailed below.

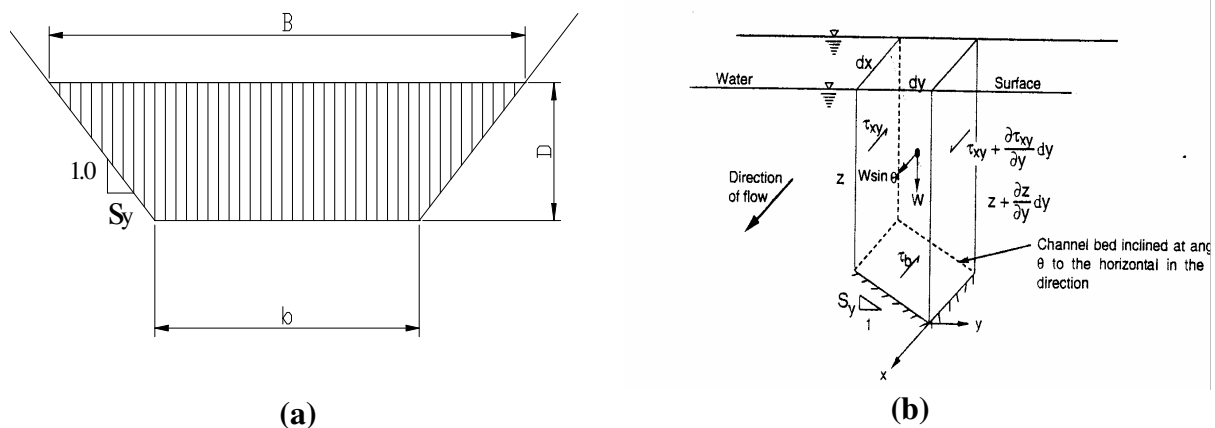


**Fig. (1): A schematic sketch of a channel division into a finite number of small vertical elements**

In Eqn. (1), the downstream component of the weight of a unit value of water (term 1) is assumed to be balanced by frictional bed shear (term 2) and lateral shear (term 3) only. The value of bed shear stress ( $\tau_b$ ) can be expressed by:

$$\tau_b = \frac{f}{8} \cdot \rho \cdot u^2 = \frac{f}{8} \cdot \rho \cdot \frac{q^2}{z^2} \quad (2)$$

where  $q$  = discharge per unit width,  $f$  = Darcy-Weisbach friction factor,  $u$  = mean velocity through the element,  $z$  = local depth measured normal to the channel bed and  $\rho$  = water density.

The value of the lateral shear stress ( $\tau_{xy}$ ), term 3 in Eqn. (1), can be expressed by:

$$\tau_{xy} = \mu \cdot \frac{\partial u}{\partial y} \quad (3)$$

where  $\mu$  = absolute viscosity.

Then this term can be formulated as follow:

$$\frac{1}{\rho} \cdot \frac{\partial(z \cdot \tau_{xy})}{\partial y} = \frac{1}{\rho} \cdot \frac{\partial(z \cdot \mu \cdot \frac{\partial u}{\partial y})}{\partial y} = \frac{1}{\rho} \cdot \frac{\partial(\mu \cdot \frac{\partial q}{\partial y})}{\partial y} = \frac{\partial}{\partial y} \left[ \varepsilon \cdot \frac{\partial q}{\partial y} \right] \quad (4)$$

where  $\varepsilon$  = eddy viscosity and the other parameters as defined before.

Now by substituting Eqns. (2) and (4) into Eqn. (1) the following expression for describing the unit discharge distribution across the channel is obtained.

$$g \cdot S \cdot z - B_* \cdot \frac{f}{8} \cdot \frac{q^2}{z^2} + \frac{\partial}{\partial y} \left( \varepsilon \cdot \frac{\partial q}{\partial y} \right) = 0.0 \quad (5)$$

A solution of this equation is possible with the addition of non-slip boundary conditions ( $q = 0$ ) at the outer boundaries of the channels. The numerical solution of Eqn. (5) is obtained using a finite difference approximation and the solution of the resulting system of non-linear equations is performed using the Newton-Raphson method. In Eqn. (5) all the terms except the Darcy-Weisbach friction factor ( $f$ ) and the eddy viscosity coefficient ( $\varepsilon$ ) can be evaluated.

A simple but reliable eddy viscosity model is used in Eqn. (5).

$$\varepsilon = NEV \cdot u_* \cdot z \quad (6)$$

where  $u_* = \sqrt{g \cdot z \cdot S}$  = local shear velocity (m/s); and  $NEV$  = user-specified non-dimensional eddy viscosity coefficient, usually taken as approximately 0.16, Darby and Thorne [15]; Darby [16] assumed it as a uniform value across the channel.

To apply the flow model for predicting the distribution of the unit discharge for a specified water-surface elevation, it is necessary to estimate local Darcy-Weisbach friction factor at each computational node across the wetted perimeter, accounting for sediment roughness elements or vegetation roughness elements. A procedure developed by Masterman and Thorne [17] is used herein to do this. Their method is based on the physically based Colebrook-White equation.

$$\frac{1}{\sqrt{f}} = a + c \cdot \log \frac{z}{k} \quad (7)$$

where  $k$  = local roughness height (m);  $c$  = coefficient assumed to take the value of Von Karman coefficient (0.4); and  $a$  = coefficient that is a function of the cross-sectional shape of the channel.

For rough bed, Masterman and Thorne [17] suggest that Hey's [18] calibration of Eqn. (7) offers reasonable predictive ability, so that;

$$\frac{1}{\sqrt{f}} = 2.03 \log \frac{a_s z}{3.5k} \quad (8)$$

where  $z$  = local flow depth;  $k$  = local roughness height; and  $a_s$  = shape-correction factor given by Hey [18], and

$$a_s = 11.1 (R/D)^{-0.314} \quad (9)$$

where  $R$  = hydraulic radius and  $D$  = the maximum water depth.

For nodes with vegetation, flexible vegetation approach is adopted. Several researchers, Kouwen [19] and Kouwen and Li [20] have shown that resistance to flow in channels with flexible vegetation can be based on a relative roughness approach similar to the widely accepted resistance relationships developed for rigid roughness in pipes and open channels (e.g., Eqns. 7-9 in this paper), with the roughness height related to stem properties. However, vegetation bends when subjected to shear, adding the requirement that the roughness height is a function of flow parameters as well. Kouwen [19] demonstrated that the significant stem properties are the stem density  $M$  and flexural rigidity in bending, given by  $J = EI$ , where  $E$  is the stem's modulus of elasticity, and  $I$  is the stem area's second moment of inertia. In laboratory experiments of flow over flexible plastic strips, where the values of  $M$ ,  $E$  and  $I$  are readily measurable, Kouwen and Li [20] showed that the roughness height varies as a function of the amount of drag exerted by the flow:

$$k = 0.14h \left( \frac{\left( \frac{MEI}{\tau} \right)^{0.25}}{h} \right)^{1.59} \quad (10)$$

where  $h$  = local height of the strips (m); and  $\tau$  = local boundary shear stress ( $\text{N/m}^2$ ). The value of the roughness height obtained using Eqn. (10) can be substituted into a relative roughness equation (e.g. Eqn. 7) to obtain the friction factor.

Unfortunately, for natural vegetation, it is not so easy to measure  $M$ ,  $E$ ,  $I$ , due to the heterogeneity of natural vegetation. Instead Kouwen and his coworkers viewed the combined effect of the product of  $M$ ,  $E$ , and  $I$  as a single quantifiable parameter called  $MEI$ . According to Kouwen [19], the combined term  $MEI$  indicates that an increase in the number of stems  $M$  per unit area has an effect similar to increasing the stiffness  $EI$  of individual elements. The use of the single term  $MEI$  to reflect the overall resistance to deformation of vegetation as a result of a flow passing over it is, therefore, justified and this parameter is obtained, Kouwen [19], using the following empirical relationship for green-growing grass;

$$MEI = 319h^{3.3} \tag{11}$$

Eqns. (5) to (11) have been implemented in a computer program written by FORTRAN language that provides estimates of unit discharge of a channel of a specified cross-section geometry and gradient, bed material size and/or vegetation height for the channel bed and side banks. The cross section is divided into a number of computational nodes as a precursor to the numerical solution of Eqn. (5). Two hundred computational nodes are used to ensure satisfactory numerical performance, Mohamed [1].

By using finite difference method, Eqn. (5) can be converted from differential form to algebraic form as follows:

$$gS_{z_i} - B_* \frac{f_i q_i^2}{8z_i^2} + \epsilon_i \left( \frac{q_{i-1} - 2q_i + q_{i+1}}{\Delta y^2} \right) + (\epsilon_i - \epsilon_{i-1}) \frac{q_i - q_{i-1}}{\Delta y^2} = 0 \tag{12}$$

for node number  $i$  from 1 to  $N$ .

This non-linear equation is solved using Taylor series by assuming initial value for  $q_i$ .

### 3. MODEL APPLICATIONS

To study the effect of variation of wetted perimeter roughness due to growth of vegetation, a number of numerical experiments (about 65 runs) were performed on three patterns of channel vegetation as shown in Fig. (2).

Pattern I: Vegetation on bed and side banks with equal height.

In this case, the channel is completely infested by submerged weeds.

Pattern II: Vegetation on bed with alluvial side banks.

In this case, both canal banks are assumed to be cut by mechanical means.

Pattern III: Vegetation on side banks with alluvial bed.

For each pattern, the ratio of channel bed width to water depth ( $b/D$ ) was changed in the range from three to fourteen. The vegetation height was changed in the range from 0.2 to 1.0 m of flexible vegetation. The side bank slope ( $S_y$ ) was changed three times (1.0:1.0, 1.5:1.0, 2.0:1.0 horizontal to vertical) and the longitudinal bed slope was changed in the range from 5 cm/Km to 15 cm/Km. Table (1) shows the different variables used in this study.

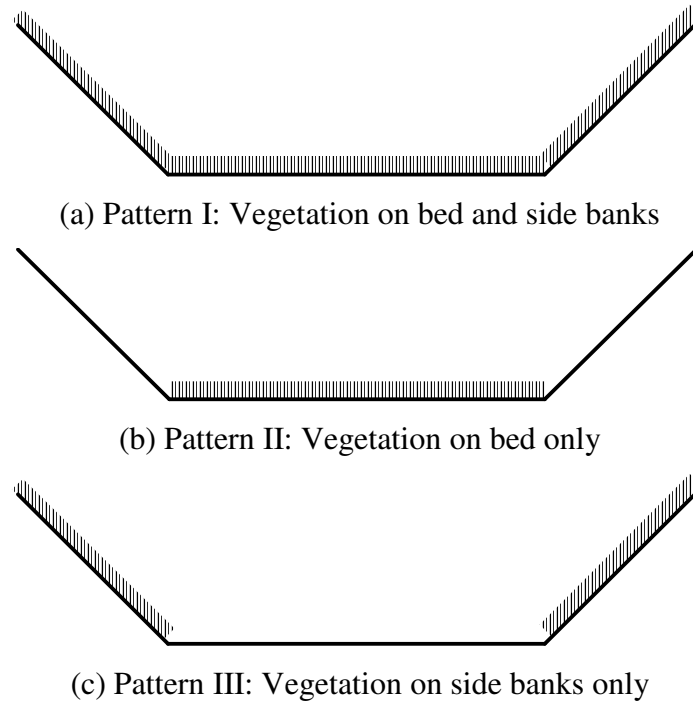


Fig. (2): Vegetation distribution along the wetted perimeter

Table (1): Range of variables used in the computations

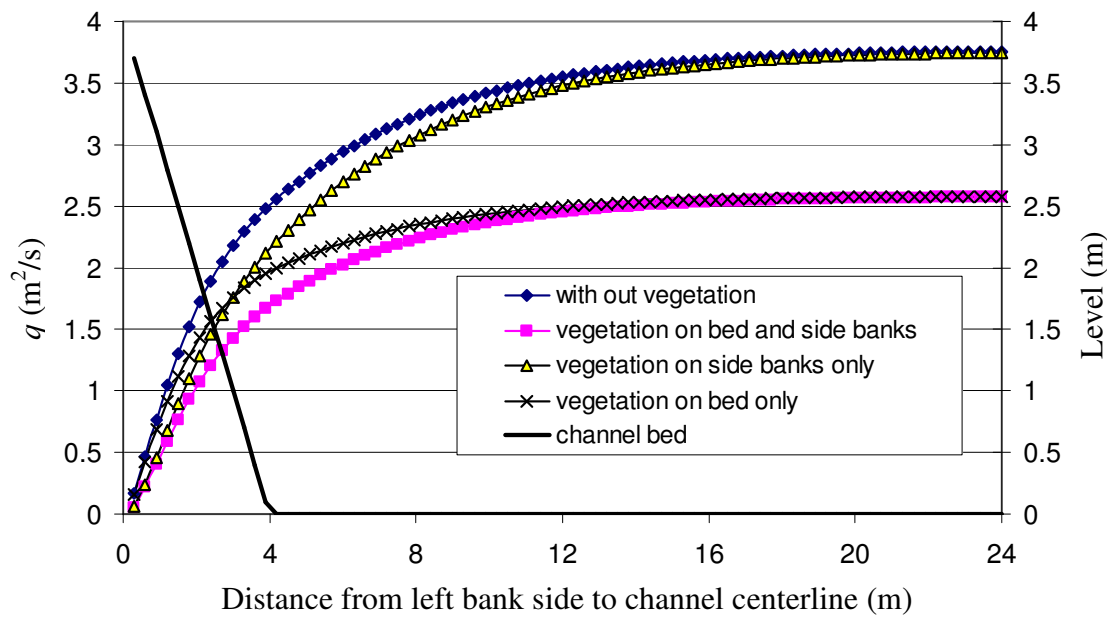
Parameter	Symbol	Value	Range		Units
			From	To	
Bed width to water depth ratio	$b/D$	varied	3	14	-
Longitudinal bed slope	$S_0$	varied	5	15	cm/Km
Side banks slope	$S_y$	varied	1.0	2.0	-
Bed vegetation height	$h_b$	varied	0.2	1.0	m
Side banks vegetation height	$h_s$	varied	0.2	1.0	m
Mean grain size	$d_b$ or $d_s$	0.015	-	-	cm

Figure (3) shows the lateral variation of unit discharge for different vegetation distribution patterns at  $b/D$  value equal to 10 for side bank slope equal to 1.0 and vegetation height equal to 0.4 m. From this figure, it is noticeable that the variation in vegetation distribution patterns affects the distribution of the unit discharge where the



higher affected pattern is for vegetation in both bed and side banks and the lower affected is for vegetation on side banks only.

Also, Fig. (4) shows the effect of variation in vegetation height between bed and side banks on the unit discharge distribution. From this figure, it is noticeable that the higher discharge occurs at bed vegetation height half the side bank vegetation height and the lower is for bed vegetation height two times the side banks vegetation height.



**Fig. (3): Lateral variation in discharge for different vegetation distribution patterns at  $b/D = 10$  and vegetation height,  $h = 0.4$  m**

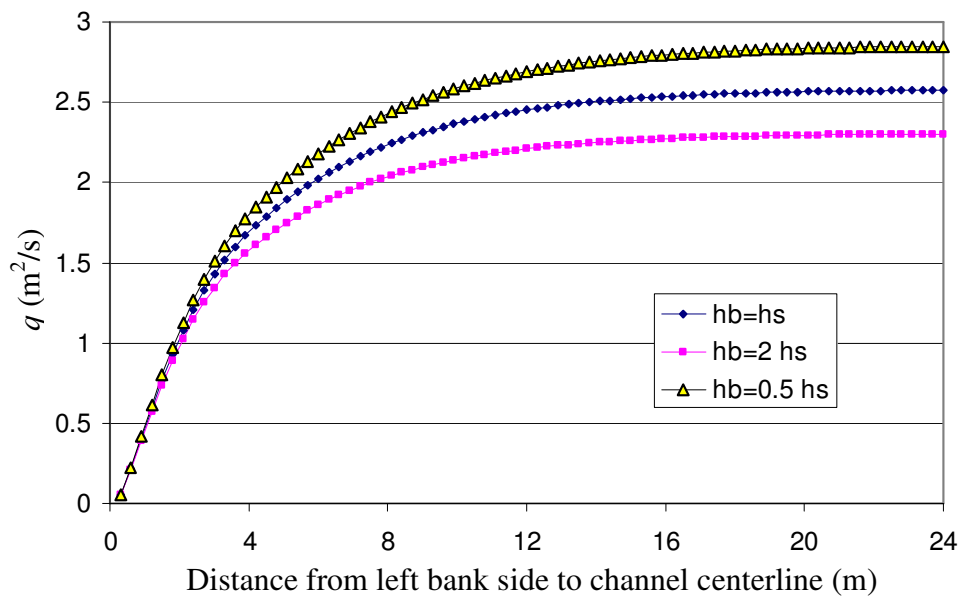


**Fig. (4): Lateral variation in discharge for different heights of bed vegetation at  $b/D = 10$  and  $h_s = 0.4$  m for side bank slope equal to 1.0**

**Pattern I: Vegetation on bed and side banks with equal heights:**

Figure (5) shows values of the equivalent Manning roughness coefficient due to vegetation on both bed and side banks to Manning roughness values due to grain size uniformly distributed along the cross-section ratio ( $n_e / n_o$ ) versus vegetation height to mean water depth ratio ( $h / D$ ) for different side bank slopes and bed width to depth ratio ( $b / D$ ) at equal vegetation on bed and side banks. From that figure, it is noticeable that  $n_e / n_o$  ratio increases by increasing of  $h / D$  and all the data points clustered around a curve, which may be expressed in the form:

$$\frac{n_e}{n_o} = \left( -5.88 \left( \frac{h}{D} \right)^2 + 4.27 \left( \frac{h}{D} \right) + 1 \right) \frac{S}{S_0} \quad R^2 = 0.967 \quad (13)$$

where  $S$  is the longitudinal channel slope with vegetation and  $S_0$  is the longitudinal slope at no vegetation.

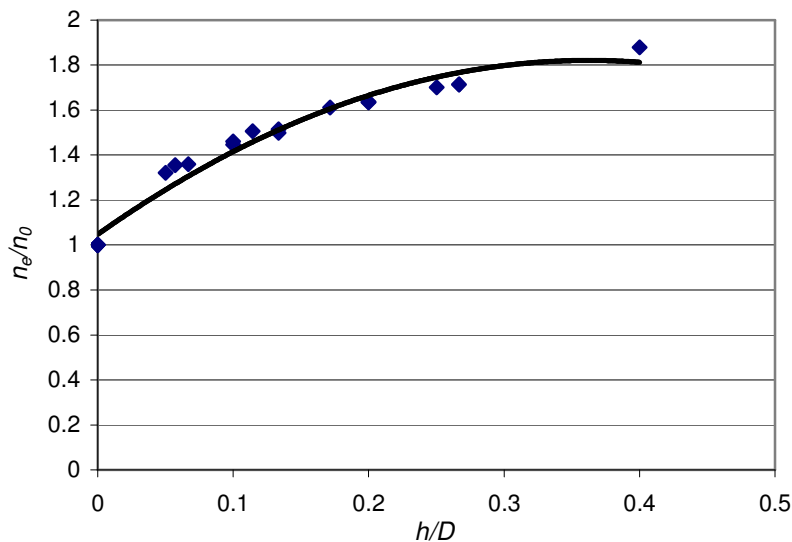


**Fig. (5): Values of  $n_e / n_o$  versus  $h / D$  for different side bank slopes and  $b / D$  ratio at equal vegetation on bed and side banks**

In Fig. (6), ratio of vegetated channel discharge to non-vegetated channel discharge ( $Q / Q_o$ ) was drawn versus vegetation height to water depth ratio ( $h / D$ ) for different side bank slopes and bed width to depth ratio ( $b / D$ ) at equal vegetation on bed and side banks. From that figure, it is noticeable that  $Q / Q_o$  ratio decreases by increasing of  $h / D$  and all the data points clustered around a curve, which may be expressed in the form:

$$\frac{Q}{Q_0} = 4.77 \left( \frac{h}{D} \right)^2 - 2.83 \left( \frac{h}{D} \right) + 1.0 \quad R^2 = 0.924 \quad (14)$$

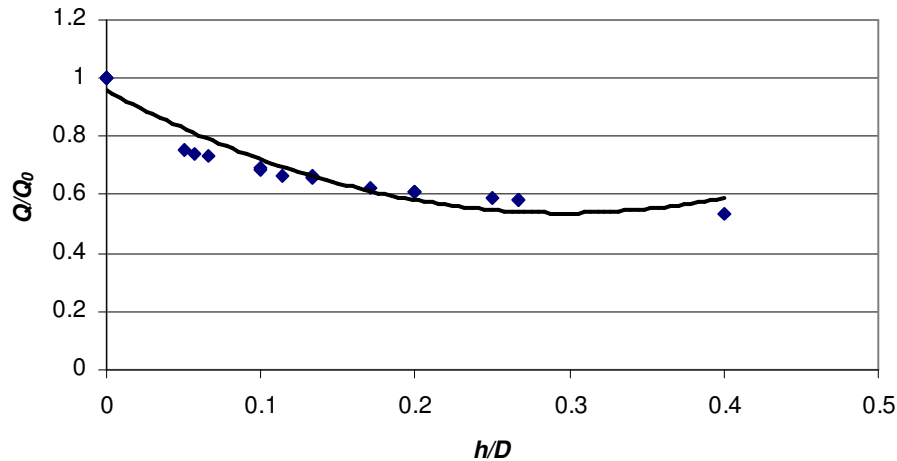


**Fig. (6): Values of  $Q/Q_0$  versus  $h/D$  for different side bank slopes and  $b/D$  ratio at equal vegetation on bed and side banks**

### Pattern II: Vegetation on bed with alluvial side banks

To show the effect of vegetation on bed only, Fig. (7) shows the relation of the dimensionless equivalent vegetated channel Manning roughness coefficients  $n_e/n_o$  versus the ratio of bed vegetation height to water depth  $h_b/D$  for different values of channel bed width to water depth ratios  $b/D$ . From that figure, it is noticeable that the equivalent Manning roughness coefficient due to bed vegetation increases by increasing of both  $h_b/D$  and  $b/D$  ratios and the side bank slopes have no effect on it. The data for each value of bed width to water depth ratio ( $b/D$ ) clustered around a curve, which may be expressed in the form:

$$\frac{n_e}{n_o} = A_1 \left( \frac{h_b}{D} \right)^2 + A_2 \left( \frac{h_b}{D} \right) + 1 \quad (15)$$

where  $A_1$  and  $A_2$  are coefficients depending on the bed width to water depth ratio ( $b/D$ ). Values of  $A_1$  and  $A_2$  were obtained from regression analysis for each value of  $b/D$ .

The correlation between  $A_1$ ,  $A_2$  and  $b/D$  may be given in the form:

$$A_1 = 0.15 \left( \frac{b}{D} \right)^2 - 3.11 \left( \frac{b}{D} \right) + 5.64 \quad (16-a)$$

$$A_2 = -0.037 \left( \frac{b}{D} \right)^2 + 0.9 \left( \frac{b}{D} \right) - 0.4 \quad (16-b)$$

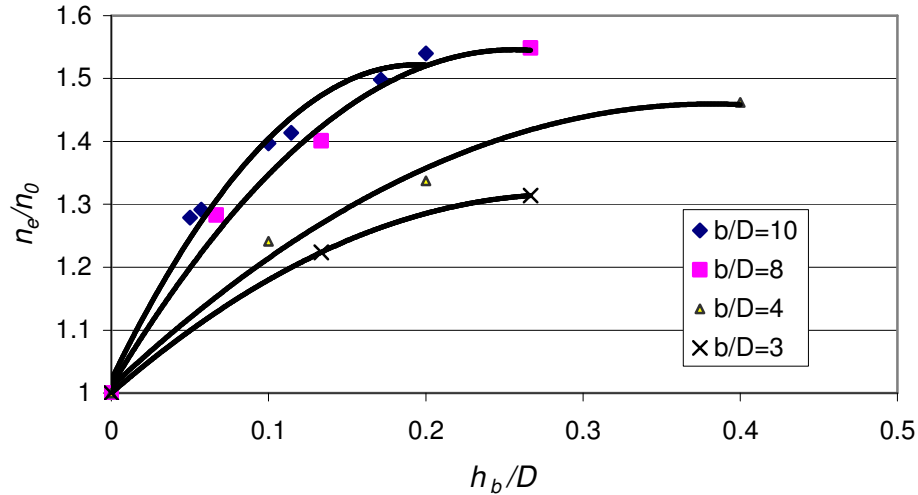


**Fig. (7): Values of  $n_e/n_o$  versus  $h_b/D$  for different side bank slopes and  $b/D$  ratio at vegetation on bed only**

In Fig. (8), ratio of bed vegetated channel discharge to non-vegetated channel discharge ( $Q/Q_o$ ) was drawn versus bed vegetation height to water depth ratio ( $h_b/D$ ) for different values of bed width to water depth ratio ( $b/D$ ). From that figure, it is noticeable that  $Q/Q_o$  ratio decreases by increasing of  $h_b/D$  and  $b/D$  ratios. The data for each value of bed width to water depth ratio ( $b/D$ ) clustered around a curve, which may be expressed in the form:

$$\frac{Q}{Q_0} = A_3 \left( \frac{h_b}{D} \right)^2 + A_4 \left( \frac{h_b}{D} \right) + 1 \quad (17)$$

where  $A_3$  and  $A_4$  are coefficients depending on the bed width to water depth ratio ( $b/D$ ).

The correlation between  $A_3$ ,  $A_4$  and  $b/D$  may be given in the form:

$$A_3 = -0.14 \left( \frac{b}{D} \right)^2 + 2.78 \left( \frac{b}{D} \right) - 4.86 \quad (18-a)$$

$$A_4 = 0.032 \left( \frac{b}{D} \right)^2 - 0.69 \left( \frac{b}{D} \right) + 0.165 \quad (18-b)$$

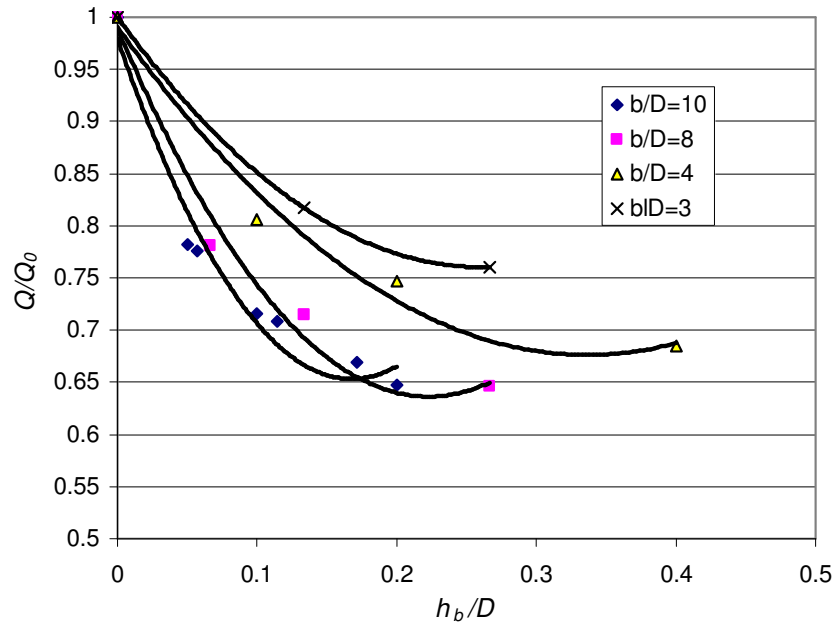


**Fig. (8): Values of  $Q/Q_0$  versus  $h_b/D$  for different side bank slopes and  $b/D$  ratio at vegetation on bed only**

### Pattern III: Vegetation on side banks with alluvial bed

To show the effect of vegetation on side banks only, Fig. (9) shows the relation of the dimensionless equivalent vegetated channel Manning roughness coefficients  $n_e/n_0$  versus the ratio of side banks vegetation height to water depth  $h_s/D$  for different values of channel bed width to water depth ratios  $b/D$ . From that figure, it is noticeable that the equivalent Manning roughness coefficient due to bed vegetation increases by increasing of both  $h_s/D$  and  $b/D$  ratios and the side bank slope have no effect on it. The data for each value of bed width to water depth ratio ( $b/D$ ) clustered around a curve, which may be expressed in the form:

$$\frac{n_e}{n_0} = A_5 \left( \frac{h_s}{D} \right)^2 + A_6 \left( \frac{h_s}{D} \right) + 1 \quad (19)$$

where  $A_5$  and  $A_6$  are coefficients depending on the bed width to water depth ratio ( $b/D$ ).

The correlation between  $A_5$ ,  $A_6$  and  $b/D$  may be given in the form:

$$A_5 = -0.14 \left( \frac{b}{D} \right)^2 + 1.98 \left( \frac{b}{D} \right) - 8.4 \quad (20-a)$$

$$A_6 = 0.044 \left( \frac{b}{D} \right)^2 - 0.76 \left( \frac{b}{D} \right) + 4.0 \quad (20-b)$$

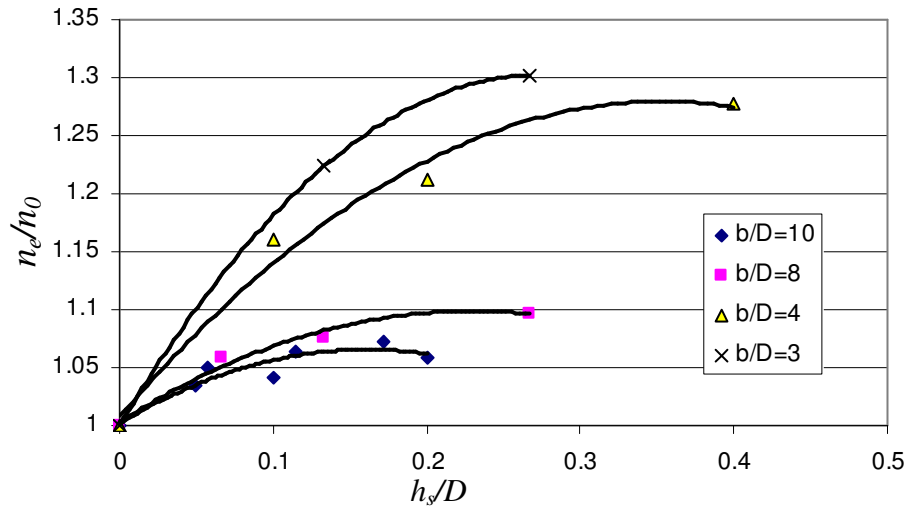


**Fig. (9): Values of  $n_e/n_0$  versus  $h_s/D$  for different side bank slopes and  $b/D$  ratio at vegetation on side banks only**

Finally, in Fig. (10), ratio of side banks vegetated channel discharge to non-vegetated channel discharge ( $Q/Q_0$ ) was drawn versus side banks vegetation height to water depth ratio ( $h_s/D$ ) for different values of bed width to water depth ratio ( $b/D$ ). From that figure, it is noticeable that  $Q/Q_0$  ratio decreases by increasing of  $h_s/D$  and  $b/D$  ratios. The data for each value of bed width to water depth ratio ( $b/D$ ) clustered around a curve, which may be expressed in the form:

$$\frac{Q}{Q_0} = A_7 \left( \frac{h_s}{D} \right)^2 + A_8 \left( \frac{h_s}{D} \right) + 1 \quad (21)$$

where  $A_7$  and  $A_8$  are coefficients depending on the bed width to water depth ratio ( $b/D$ ).

The correlation between  $A_7$ ,  $A_8$  and  $b/D$  may be given in the form:

$$A_7 = 0.13 \left( \frac{b}{D} \right)^2 - 1.82 \left( \frac{b}{D} \right) + 7.68 \quad (22-a)$$

$$A_8 = -0.035 \left( \frac{b}{D} \right)^2 + 0.6 \left( \frac{b}{D} \right) - 3.28 \quad (22-b)$$

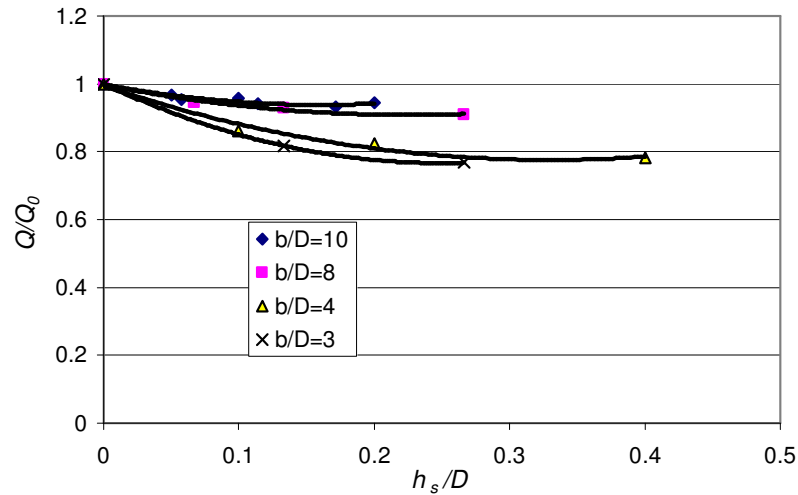


**Fig. (10): Values of  $Q/Q_0$  versus  $h_s/D$  for different side bank slopes and  $b/D$  ratio at vegetation on side banks only**

#### 4. APPLICABILITY OF THE MODEL TO ACTUAL VEGETATED CANAL

The proposed model was applied for two actual field cases found in literature. The first one is for the canal cross-section wholly covered by submerged weeds, while the second case is after cutting vegetation along both canal banks. These study cases are for Ismailia canal, which is one of main canals in Eastern Delta of river Nile (Egypt), for more details about the geometric properties, measured data and computed parameters concerning the two cases can be found in Bakry [2]. Measurements were taken in the lower reach of Ismailia canal at five different stations when the whole canal cross-section covered by submerged weeds and when the bed only covered by vegetation, respectively. Figure (11) shows a comparison between the discharges computed using the present method and the measured one. It is noticeable that there is a good agreement between the measured and computed discharge with slightly overpredicted discharges computed using the model but this may be due to the accumulative errors in computing the parameters entering in discharge computation and it is in the acceptable range. Also, Fig. (12) shows a comparison between the actual equivalent Manning's roughness and the computed one. It can be seen fairly good agreement between the actual roughness coefficient and that computed using the present method.

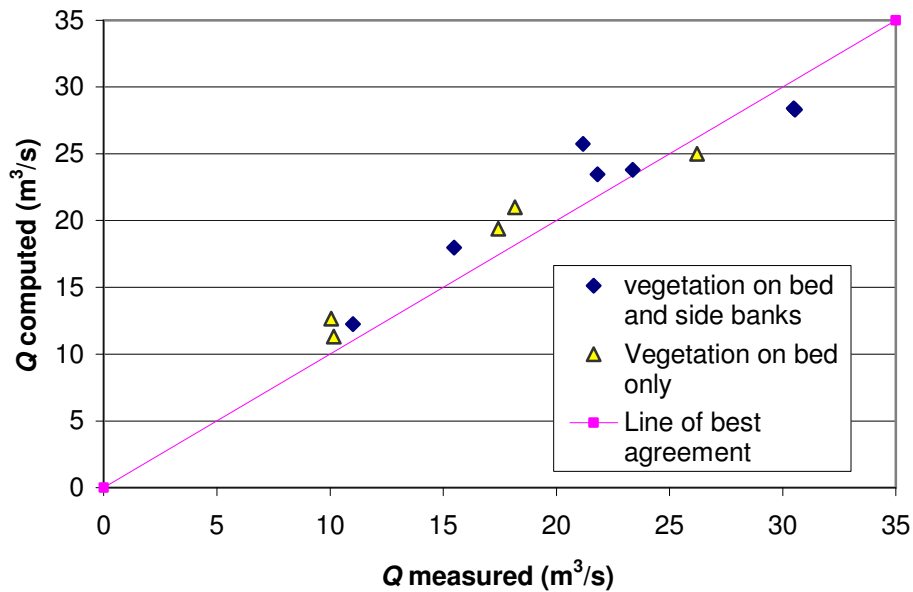


Fig. (11): A comparison between the measured and computed discharge

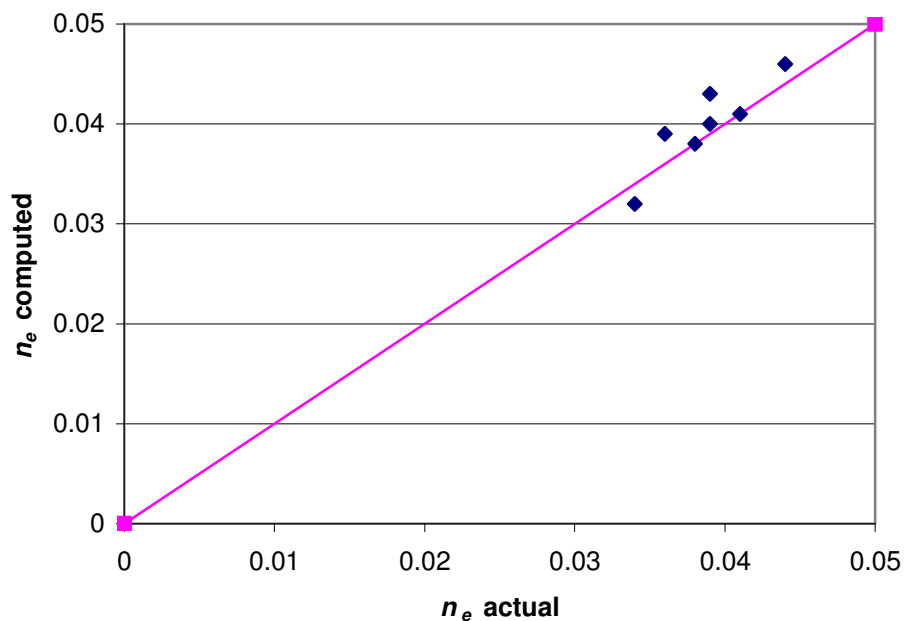


Fig. (12): A comparison between the actual equivalent Manning's roughness coefficient and the computed one

## 5. CONCLUSIONS

1. To minimize the discrepancy in total conveyance value for flow in channel with variation in vegetated roughness through the wetted perimeter, a new subdivision method take into account the momentum transfer and lateral shear stress distribution between the elements was introduced.



2. A numerical model that predicts the flow capacity of a channel with varying vegetation cover through perimeter has been developed.
3. Three patterns of flexible vegetation of channel roughness distribution were studied.
4. To provide the design engineer with a practical mean of generating the model results without having to run the numerical model, equations and plots based on model were developed for the total channel discharge and the equivalent Manning roughness coefficient.
5. Also, the model was applied for actual cases in the field and it was found that the model overestimates the discharge slightly.

## REFERENCES

- [1] Mohamed, H. I., (2004), "Effect of lateral variation of roughness on flow conveyance within a trapezoidal channel cross-section", *Jour. of Eng. Sciences, Assiut University*, Vol. 32, No. 5, pp. 1871-1885.
- [2] Bakry, M. F., (1996), "Impact of mechanical cutting on the channel roughness", *Water Resour. Manag.*, Vol. 10, No. 6, pp. 479-486.
- [3] Bakry, M. F., (1992), "Effect of submerged weeds on the design procedure of earthen egyptian canals", *Irrig. & Drain. Syst.*, Vol. 6, No. 3, pp. 179-188.
- [4] Salama, M. M., and Bakry, M. F., (1992), "Design of earthen vegetated open channels", *Water Resour. Manag.*, Vol. 6, No. 2, pp. 149-159.
- [5] U.S. Army Corps of Engineers, (1994), "Methods for predicting n values for Manning equation", EM 1110-2-1601.
- [6] Armanini, A., and Righetti, M., (1998), "Flow resistance in compound vegetated channel", *ICHE conference*.
- [7] Garbrecht, J., and Brown, G. O., (1991), "Calculation of total conveyance in natural channels", *Jour. of Hydraulic Eng.*, Vol. 117, No. 6, pp. 788-798.
- [8] Myers, W.R.C., Lyness, J.F., and Cassells, J.B. (1999), "Estimation of roughness coefficient for compound channels", *IAHR Conference, Graz, Austria*.
- [9] Rabkova, E. K., and Garanina, E. V., (2001), "Distribution of averaged local velocities in an open turbulent flow", *Water Resources*, Vol. 28, No. 5, pp. 577-580.
- [10] Liao, H., and Knight, D. W., (2007), "Analytic stage-discharge formulae for flow in straight trapezoidal open channels", *Advanc. in Water Resour.*, Vol. 30, pp. 2283-2295.
- [11] Liao, H., and Knight, D. W., (2007), "Analytic stage-discharge formulas for flow in straight prismatic channels", *Jour. of Hydr. Eng.*, Vol. 133, No. 10, pp. 1111-1122.
- [12] Zarrati, A. R., Jin, Y. C. and Karimpour, S., (2008), "Semianalytical model for shear stress distribution in simple and compound open channels", *Jour. of Hydr. Eng.*, Vol. 134, No. 2, pp. 205-215.

- [13] Lim, S. Y., and Yang, S. Q., (2005), "Simplified model of tractive-force distribution in closed conduits", *Jour. of Hyd. Eng.*, Vol. 131, No. 4, pp. 322-329.
- [14] Lambert, M. F., and Sellin, R. H. J., (1996), "Discharge prediction in straight compound channels using the mixing length concept", *Jour. of Hydraulic Research*, Vol. 34, No. 3, pp. 381-395.
- [15] Darby, S. E., and Thorne, C. R., (1996), "Predicting stage-discharge curves in channels with bank vegetation", *Jour. of Hydraulic Eng.*, Vol. 122, No. 10, pp. 583-586.
- [16] Darby, S. E., (1999), "Effect of riparian vegetation on flow resistance and flood potential", *Jour. of Hyd. Eng.*, Vol. 125, No. 5, pp. 443-454.
- [17] Masterman, R., and Thorne, C. R., (1992), "Predicting influence of bank vegetation on channel capacity", *J. Hydr. Engrg.*, Vol. 118, No. 7, pp. 1052-1058.
- [18] Hey, R. D., (1979), "Flow resistance in gravel-bed rivers", *J. Hydr. Div., ASCE*, Vol. 105, No. 4, pp. 365-379.
- [19] Kouwen, N., (1992), "Modern approach to design of grassed channels", *Jour. of Irrig. and Drain. Eng.*, Vol. 118, No. 5, pp. 733-743.
- [20] Kouwen, N. and Li, R., (1980), "Biomechanics of vegetative channel linings", *Jour. of Hyd. Div.*, Vol. 106, No. HY6, pp. 1085-1102.